

E4-2026-27

A. D. Efimov<sup>1,2,\*</sup>, I. V. Koval<sup>1,\*\*</sup>, I. N. Izosimov<sup>3,\*\*\*</sup>

DESCRIPTION OF HIGH-SPIN STATES  
IN EVEN PLUTONIUM ISOTOPES

Submitted to “Physical Review C”

---

<sup>1</sup> Admiral Makarov State University of Maritime and Inland Shipping,  
St. Petersburg, Russia

<sup>2</sup> Ioffe Physical-Technical Institute, Russian Academy of Sciences,  
St. Petersburg, Russia

<sup>3</sup> Joint Institute for Nuclear Research, Dubna, Russia

\* E-mail: efimov98@mail.ru

\*\* E-mail: lonai1104@list.ru

\*\*\* E-mail: izosimov@jinr.ru

Ефимов А. Д., Коваль И. В., Изосимов И. Н.

E4-2026-27

Описание высокоспиновых состояний в четных изотопах плутония

Выполнено систематическое исследование вращательных полос в четных ядрах  $^{236-244}\text{Pu}$  в рамках феноменологической и микроскопической версий модели взаимодействующих бозонов (IBM), а также модели Харриса с переменным моментом инерции. Микроскопическое описание коллективных состояний основано на фононном подходе с использованием сферического базиса Вудса–Саксона, что позволяет на единой основе описывать основную,  $\beta$ - и  $\gamma$ -полосы. Для ядер  $^{238-244}\text{Pu}$  учтены высокоспиновые двухквизичастичные моды возбуждений. Для  $^{242,244}\text{Pu}$  получено пересечение полос, проявляющееся через бэкбендинг; для  $^{238,240}\text{Pu}$  пересечение отсутствует, однако учет высокоспиновых мод существенно улучшает описание энергий, что наиболее отчетливо проявляется в значениях моментов инерции.

Работа выполнена в Лаборатории ядерных реакций им. Г. Н. Флерова ОИЯИ.

Препринт Объединенного института ядерных исследований. Дубна, 2026

Efimov A. D., Koval I. V., Izosimov I. N.

E4-2026-27

Description of High-Spin States in Even Plutonium Isotopes

A systematic study of rotational bands in even-even  $^{236-244}\text{Pu}$  nuclei is performed within the phenomenological and microscopic versions of the interacting boson model (IBM), as well as within the Harris model with variable moment of inertia. The microscopic description of collective states is based on the phonon approach with a spherical Woods–Saxon basis, allowing a unified description of the ground,  $\beta$ , and  $\gamma$  bands. For  $^{238-244}\text{Pu}$ , high-spin two-quasiparticle excitation modes are taken into account. For  $^{242,244}\text{Pu}$ , a band crossing manifesting itself as backbending is obtained; for  $^{238,240}\text{Pu}$ , no crossing occurs, but the inclusion of high-spin modes significantly improves the energy description, especially in the moments of inertia.

The investigation has been performed at the Flerov Laboratory of Nuclear Reactions, JINR.

Preprint of the Joint Institute for Nuclear Research. Dubna, 2026

## INTRODUCTION

It was noted in [1] that among all even-even nuclei with  $Z \geq 90$  for which experimental data are available, the backbending phenomenon in the moment of inertia as a function of the square of the rotational frequency is observed only for  $^{242,244}\text{Pu}$ . References to works using various microscopic approaches describing this phenomenon in  $^{242,244}\text{Pu}$  are also given there. These include microscopic approaches using self-consistent calculations in a deformed single-particle basis [2, 3]. The relativistic Hartree–Bogoliubov theory with rotational motion was also used in the theoretical study of these nuclei [4]. It was noted that, at that time, the generation of energy density functionals did not achieve the same accuracy in describing single-particle state energies as models based on phenomenological Woods–Saxon or Nilsson potentials.

In the mentioned work [1], the energies of yrast bands in even-even isotopes of Pu, Cm, Fm, and No were analyzed. This was done within the phenomenology of the interacting boson model IBM [5, 6], where the Hamiltonian parameters are adjusted to best reproduce the energies of collective states. The adjustable parameters also included the maximum number of bosons  $\Omega$ , and this number turned out to be large, up to 36. The Harris model [7] was also used in its phenomenological aspect. Only for two nuclei,  $^{244}\text{Pu}$  and  $^{248}\text{Cm}$ , a microscopic model oriented toward the IBM and capable of describing band crossing was applied. Taken together, this made it possible to develop a criterion for estimating the contribution of noncollective components as spin increases in yrast states. In the present work, all even-even Pu isotopes are considered on a microscopic basis. For those nuclei where band crossing does not occur, taking into account high-spin excitation modes nevertheless turns out to be important for describing the energies of high-spin states.

The theoretical model, or theory, used in this work considers elementary excitation modes through a phonon representation. Phonons are treated as a superposition of two-quasiparticle components. The phonons are then mapped onto ideal bosons according to the method used in IBM [5]. The boson Hamiltonian is not expressed in terms of  $Q$  and  $P$  operators but rather in terms of products of  $d$  and  $s$  operators in normal order. In this case, if the parameter preceding  $d^+ \cdot d$  is positive, it is called the  $d$ -boson energy. If it is negative, which is characteristic of deformed nuclei with a rotational character of the spectrum, it can simply be considered as one of the boson parameters of the Hamiltonian. If a negative phonon energy is possible in the Tamm–Dancoff approximation, then for the traditional quasiparticle random-phase approximation (QRPA) this turns out to be beyond the phase transition.

Therefore, a modification of QRPA was implemented. This modification leads to a significant reduction of correlations in the ground state.

A spherical Woods–Saxon single-particle potential with the parameterization from [8] is used. The number of nucleons of each type was taken to be 40. The rotational character of the spectrum arises as a result of the  $d$ -boson interaction.

If a deformed single-particle basis is used, the phonons constructed from two-quasiparticle configurations yield, in particular,  $\beta$  and  $\gamma$  vibrations, and the corresponding bands are built on them. The ground-state band represents rotational states built on the phonon vacuum. This approach cannot be used for a microscopic calculation of the IBM parameters. Therefore, the use of a spherical single-particle basis is, in the authors' view, the only acceptable one.

In order to more conveniently represent the structure of the boson wave function for a negative value of the parameter that is usually associated with the single-boson energy, we represent the boson wave functions in the basis of the irreducible representation of the  $SU(5)$  group as

$$|I\rangle = \sum_{n_d, v, \omega_\Delta} \alpha_d(n_d, v, \omega_\Delta, I) \frac{1}{\sqrt{(\Omega - n_d)!}} (s^+)^{\Omega - n_d} |n_d, v, \omega_\Delta, I\rangle, \quad (1)$$

where  $|n_d, v, \omega_\Delta, I\rangle$  are normalized functions of quadrupole bosons corresponding to the irreducible representation of the  $SU(5)$  group with a set of quantum numbers: the number of quadrupole bosons ( $n_d$ ), boson seniority ( $v$ ), and the number of its triplets ( $\omega_\Delta$ ) coupled to zero angular momentum. The  $s$  operator in Eq.(1) corresponds to a scalar boson, but in our interpretation it is not associated with an elementary excitation mode; rather, it arises from mapping the phonon  $D$  operator onto an ideal boson operator  $d$ . The normalization condition has the form

$$\langle I|I\rangle = \sum_{n_d, v, \omega_\Delta} \alpha_d^2(n_d, v, \omega_\Delta, I) = 1. \quad (2)$$

The amplitudes  $\alpha_d$  depend on the parameters of the boson Hamiltonian and are determined by diagonalization. In the simplest case, i.e., in the vibrational basis, the only amplitudes with  $\alpha_d = 1$  for the yrast band states with  $I = 0^+, 2^+, 4^+, 6^+, \dots$  correspond to configurations with  $n_d = 0, 1, 2, 3, \dots$ . As quadrupole collectivity increases, components with other values of  $n_d$  and  $v$  also appear in the states. For the  $^{244}\text{Pu}$  nucleus, the contribution of the wave function components from different  $n_d$  values for spins  $0^+$ ,  $8^+$ , and  $16^+$  is shown in Fig. 1. It is seen that for the states presented, the components are distributed approximately in the same region from  $n_d = 12$  to 22. Moreover, the maximum of the wave function as the spin of the collective state changes from  $I = 0$  to  $I = 16$  shifts only from  $n_d = 16.5$  to 18.3. The average values of  $n_d$  for collective states as a function of increasing spin are shown in Fig. 2 and, as can be seen, change significantly more slowly than in the vibrational case, where the transition from one state to the next in the yrast band is accompanied by a change in the number of quadrupole bosons by one. This

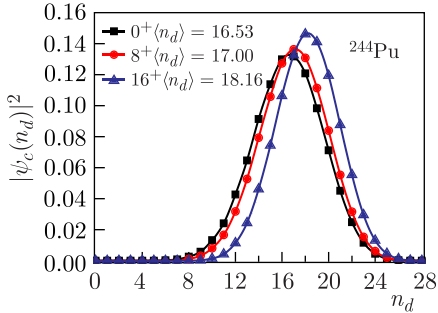


Fig. 1. Contribution to the wave functions of the  $0^+$ ,  $8^+$ , and  $16^+$  collective states in the IBM approximation of components with different  $n_d$  values

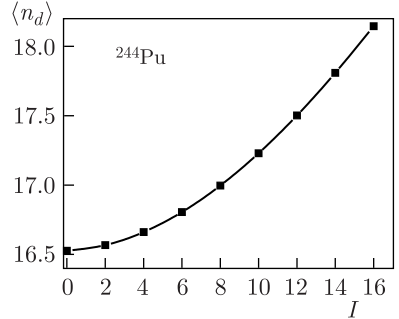


Fig. 2. Average values of quadrupole bosons  $\langle n_d \rangle$  for the  $^{244}\text{Pu}$  nucleus as a function of the spin of collective states

clearly demonstrates the fact that in the rotational case the increase in spin is mainly accompanied not by an increase in the number of quadrupole bosons, but by a recoupling of the angular momenta of those already present.

The key advantage of using a spherical single-particle potential is that its wave functions have good angular momentum from the very beginning.

The description of the rotational and vibrational character of the bands is unified within the framework characteristic of the IBM, where the structure of collective states is determined by the parameters of the boson Hamiltonian.

Here we will not repeat the exposition of the microscopic model used, which was done earlier in [9] taking into account high-spin excitation modes up to  $J \leq 10^+$ , in [10, 11] up to  $J \leq 14^+$ , and in a somewhat schematic form but with more emphasis on the physical ideas in [1]. We only note that instead of the traditional QRPA for the lowest quadrupole phonon  $D$  its modification is used. Realistic values of all IBM parameters are obtained by taking into account the coupling between states built from  $D$  phonons and states of the type  $B_J D^k$ , where  $J \leq 6$  and  $k = 0, 1, 2$ . This interaction, leading to a renormalization of the boson parameters, is particularly important for the parameters that determine the difference between the energy of the two-phonon triplet and twice the single-boson energy. The explicit inclusion of high-spin excitation modes makes it possible to quantitatively describe band crossing and the associated backbending phenomenon. The superfluidity parameters are determined from a functional that also includes the functional from which the  $D$ -phonon amplitudes are determined.

The calculation results for all considered nuclei are presented within the phenomenology of the IBM and the Harris model. The parameterization of the latter and the values of the parameters themselves are given in [1] and are not presented here.

A graphical representation of band energies turns out to be not very informative when the excitation energies as a function of spin range from 45 keV to 6 MeV. This difficulty is overcome by representing the energies in

terms of the moment of inertia as a function of the square of the frequency. This makes it possible to notice fine details in the band energies.

In contrast to [1], only Pu isotopes are considered, but for most of them the results are presented within all three approaches.

## 1. GENERAL REMARKS

The Hamiltonian is used in the following parameterization:

$$H_{\text{IBM}} = \varepsilon_d \hat{n}_d + k_1 (d^+ \cdot d^+ s s + \text{H.c.}) + k_2 ((d^+ d^+)^{(2)} \cdot d s + \text{H.c.}) + \frac{1}{2} \sum_L C_L (d^+ d^+)^{(L)} \cdot (d d)^{(L)}, \quad (3)$$

where H.c. denotes Hermitian conjugate, the dot indicates a scalar product between operators, and  $\varepsilon_d$ ,  $k_1$ ,  $k_2$ ,  $C_0$ ,  $C_2$ ,  $C_4$  are model parameters. The total boson number (or maximum number of  $d$  bosons) is denoted by  $\Omega$ .

Similarly, the  $E2$  transition operator has the form

$$\hat{T}(E2) = e^* (d^+ s + s^+ d + \chi_{E2} d^+ d)^{(2)} + e_0^* (s^+ (d^+ d)^{(0)} d + d^+ (d^+ d)^{(0)} s)^{(2)}. \quad (4)$$

Its parameters in the microscopic version are calculated according to the procedure described in [12].

The theoretical approach used in this work can be considered both microscopic and semimicroscopic. It is microscopic because both the traditional IBM parameters are calculated on the basis of effective nucleon–nucleon forces, and the interaction parameters between collective and quasiparticle excitation modes are also calculated. However, because for heavy nuclei the state energies are very sensitive to the boson parameters, as was demonstrated in [13], the boson parameters have to be slightly adjusted to best reproduce the experimental energies. This introduces an element of phenomenology into the theory, but since the parameters then remain close to the calculated values, the overall theoretical approach can be considered semimicroscopic. The parameters corresponding to IBM phenomenology and used in the microscopic calculations are given in Table 1. At the same time, the values of  $\Omega$  differ. While in phenomenology  $\Omega$  is determined from the best reproduction of experimental energies, in microscopic calculations  $\Omega$  is a calculated quantity. The parameters used in the variable moment of inertia model (VMI) are given in [1]. It should be borne in mind that in the VMI the description will always be better because its four parameters are adjusted by the least squares method, which is impossible for the IBM. Moreover, this model reproduces the energies of states that are already affected by high-spin excitation modes, but band crossing has not occurred yet. The use of the VMI provides an independent approach to describing the energies of states, which is important for understanding the behavior of both the energies in the band and the influence of noncollective excitation modes on the yrast band states.

Table 1. Parameters of the IBM Hamiltonian for the even isotopes of Pu

Nucleus	$\varepsilon_d$	$k_1$	$k_2$	$C_0$	$C_2$	$C_4$	$\Omega$
$^{236}\text{Pu}$	-0.849292	-0.061687	0.042947	0.795142	0.052083	0.025829	28
$^{238}\text{Pu}$	-0.803958	-0.056344	0.048141	0.617172	0.046336	0.028484	27
$^{238}\text{Pu}$ — for micr.	-0.742422	-0.057089	0.049427	0.556827	0.049672	0.018445	28
$^{240}\text{Pu}$	-0.628380	-0.049306	0.038750	0.699907	0.097917	0.038583	25
$^{240}\text{Pu}$ — for micr.	-0.683897	-0.049474	0.038090	0.693344	0.114566	0.039554	26
$^{242}\text{Pu}$	-0.830231	-0.061721	0.048603	0.764612	0.032435	0.040341	24
$^{242}\text{Pu}$ — for micr.	-0.745324	-0.038740	0.023057	0.058958	0.068831	0.014052	28
$^{244}\text{Pu}$	-0.804107	-0.062369	0.061048	0.596084	0.021146	0.023194	24
$^{244}\text{Pu}$ — for micr.	-0.746115	-0.041201	0.024438	0.077899	0.030130	0.014143	28
$^{246}\text{Pu}$	-0.792760	-0.060414	0.052828	0.620469	0.043172	0.029228	24

Among even-even nuclei in the actinide region, backbending is observed only for Pu isotopes. We begin the discussion with those nuclei where this effect is observed, i.e., from heavy to lighter ones. For the  $^{246}\text{Pu}$  nucleus, states are observed only up to spin  $I = 12^+$ , and it is omitted.

## 2. RESULTS OF CALCULATIONS

**2.1. Calculation for  $^{244}\text{Pu}$ .** For  $^{244}\text{Pu}$ , as seen in Fig. 3, the backbending phenomenon is most pronounced. The experimental state energies and the corresponding moments of inertia up to spins  $I = 18^+$ ,  $I = 20^+$  are well reproduced both in the VMI and in the IBM phenomenology, as can be seen from Fig. 3 and Table 2. The presented results of microscopic calculations differ somewhat from the preliminary ones presented in [1]. At the same time, the backbending itself is well reproduced up to the state with spin  $I = 28^+$ . The energies at higher spins show a significant overestimation compared to the experimental values. The simplest explanation here may be related to a high-spin four-quasiparticle excitation, for example,  $(j_{15/2}^4)^{(24^+)}$ , which is not taken into account in the calculations.

The structure of the yrast band states is shown in Fig. 4. By “coll.” we mean the sum of all components built only from  $d$  bosons, and  $b(J)$  are the components that include all possible bosons with spin  $J$ . Moreover, in each of the components there is at most one noncollective (non- $d$ ) boson. From this figure it can be seen that at spin  $I = 24^+$  a band crossing occurs, where the collective component becomes equal to the component containing  $b_{J=12^+}$  and amounts to approximately 35%. Interestingly, for  $^{244}\text{Pu}$  the experimental moment of inertia for  $2^+$  turns out to be slightly larger than that for the  $4^+$  state. This is reproduced in the microscopic calculation. This precedent shows that such a situation can occur, and therefore estimating the energy of the  $2^+$  state by extrapolating from transition energies at higher spins may not always be correct. At the same time, as can be seen from Fig. 3 and Table 2, the description of energies up to states with spin  $28^+$  is quite satisfactory.

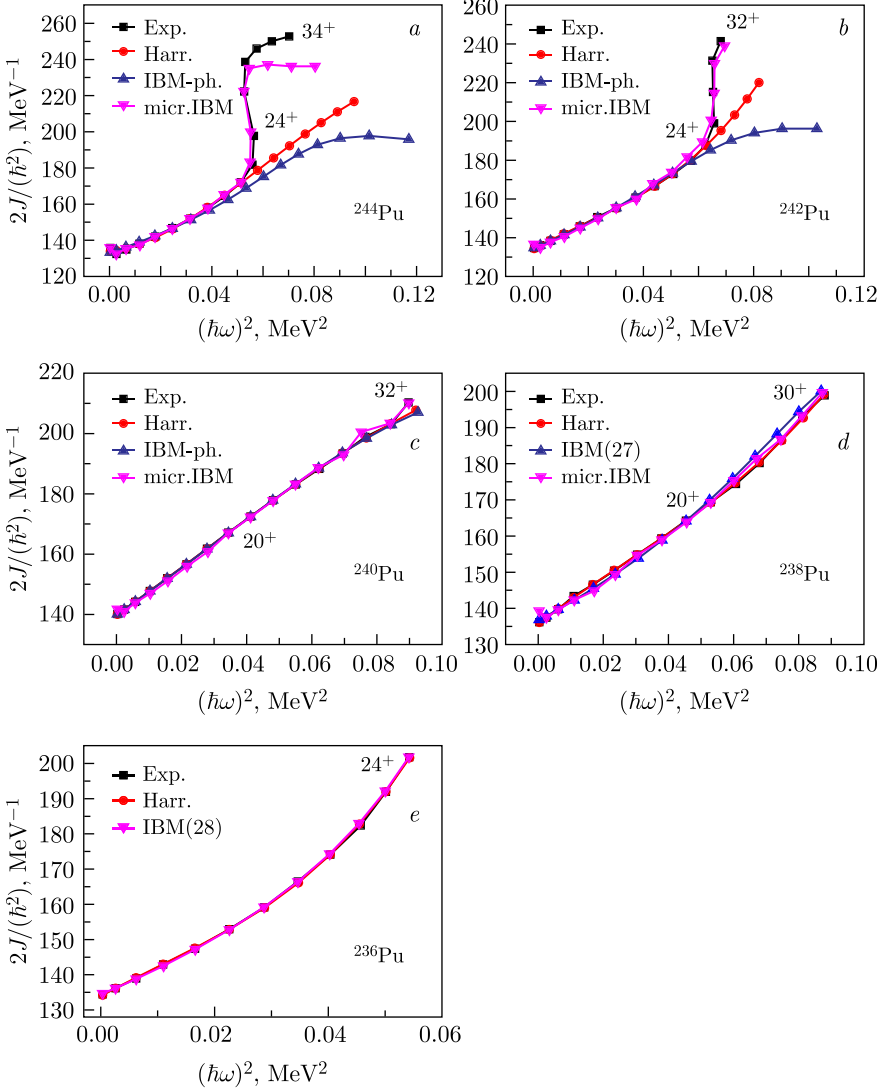


Fig. 3. Effective moments of inertia from experimental and theoretical energy values of yrast bands in Pu isotopes

Figure 3 presents the calculated  $B(E2)$  values. Despite the fact of band crossing, no dip in the  $B(E2)$  values is observed in the calculated results. This is due to the fact that the replacing band at the band crossing point has a large collective spin. That is, in the component  $b_{12+}^+|\psi(I_c)$  of the state, where the state  $\psi(I_c)$  is built only from  $d$  bosons,  $I_c = 12^+$ . The replacing

Table 2. Comparison of experimental [15] and theoretical (Harris and IBM) excitation energies (in keV) for  $^{244}\text{Pu}$ . The  $E_{\text{cal}}$  corresponds to the calculation in the Harris model, the IBM calculation uses  $\Omega = 24$

$I^\pi$	Exp.	$E_{\text{cal}}$	$E_{\text{cal}} - E_{\text{exp}}$	$E_{\text{IBM}}$	$E_{\text{IBM}} - E_{\text{exp}}$	$E_{\text{micr. IBM}}$	$E_{\text{micr. IBM}} - E_{\text{exp}}$
2+	44.2(2)	44.83	0.63	45.00	0.8	44.14	-0.06
4+	149.9(6)	149.00	-0.90	149.17	-0.73	149.82	-0.08
6+	313.0(5)	311.20	-1.80	310.59	-2.41	312.28	-0.72
8+	530.2(7)	528.68	-1.52	526.45	-3.75	530.65	0.45
10+	797.8(8)	797.21	-0.59	793.26	-4.21	798.23	0.43
12+	1111.4(9)	1111.70	0.30	1107.1	-4.3	1112.36	0.96
14+	1466.7(10)	1467.09	0.39	1464.0	-2.7	1467.59	0.89
16+	1859.2(10)	1858.88	-0.32	1859.8	0.6	1860.46	1.26
18+	2284.5(11)	2283.34	-1.16	2290.5	6	2283.92	-0.58
20+	2737.9(12)	2737.43	-0.47	2752.8	14.9	2737.32	-0.58
22+	3211.0(13)	3218.76	7.76	3243.8	32.8	3206.54	-4.46
24+	3686.3(14)	3725.45	39	3761.4	75	3676.63	-9.67
26+	4145.2(15)	4256.03	111	4305.0	160	4135.23	-9.97
28+	4606.1(17)	4809.40	203	4875.4	269	4603.12	-2.98
30+	5085.7(20)	5384.81	299	5476.0	390	5100.63	14.93
32+	5589.6(22)	5981.78	392	6113.2	524	5633.96	44.36
34+	6119.7(24)	6600.19	480	6797.4	678	6201.16	81.46

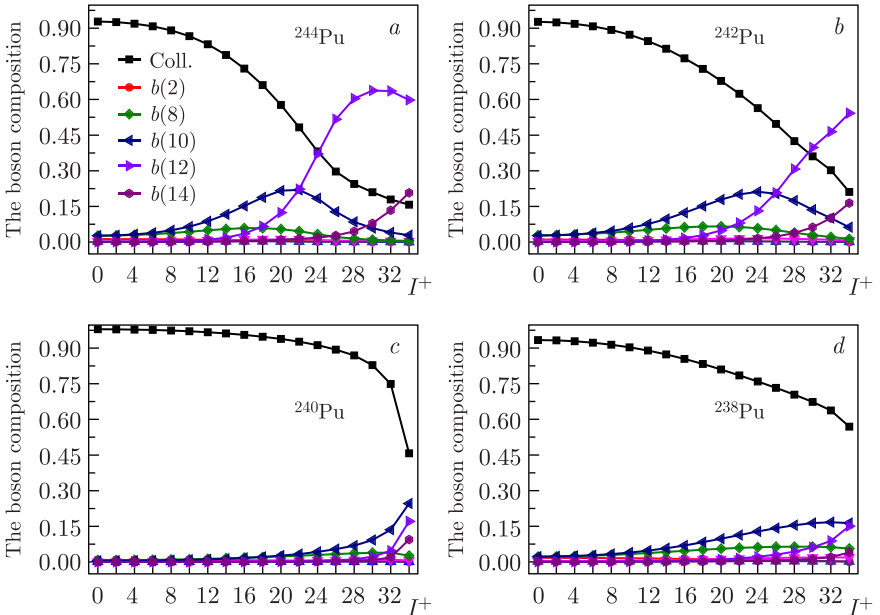


Fig. 4. Bosonic composition of wave functions; “coll.” is the total contribution from components containing only  $d$ -bosons, while  $b(J)$  are the components that additionally contain one of the  $b(J)$  bosons

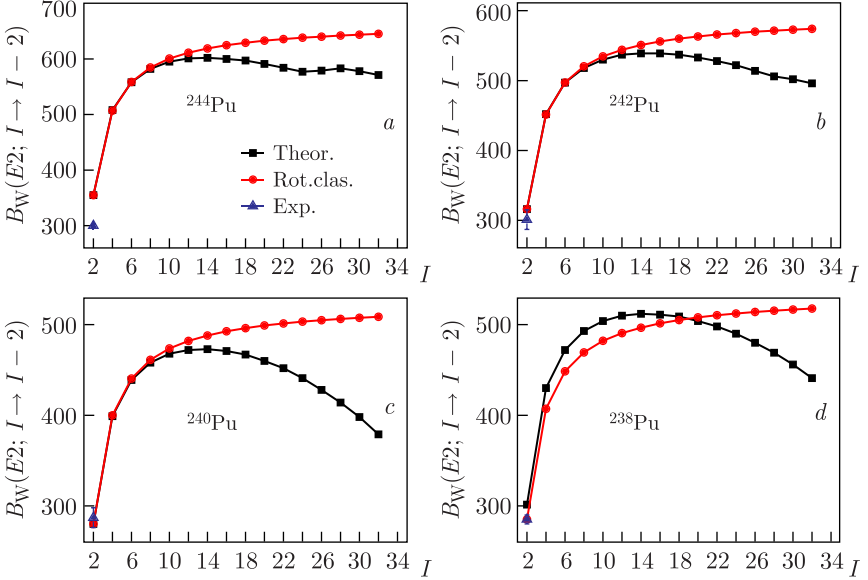


Fig. 5. The  $B(E2)$  values in single-particle units obtained from the present calculations, those from the geometric Bohr model, and the experimental values

band in the band crossing region has a significant spin of the collective part. In medium-mass nuclei, the replacing band in its collective part essentially starts from the very beginning, which gives a  $B(E2)$  value at the crossing point approximately equal to  $B(E2; 2^+ \rightarrow 0^+)$  [9, 14]. Even such a value is not a trivial result, since it requires significant mixing of the collective and quasiparticle components of the wave function. A decrease in the calculated  $B(E2)$  values is observed in the band starting from spin  $16^+$ . This is due to the presence of a cutoff factor in the  $T(E2)$  operator coming from the  $s$ -boson operator. In the classical rotational model, this factor is absent and  $B(E2)$  increases, approaching the limit  $1.875B(E2; 2^+ \rightarrow 0^+)$ . The corresponding values are also shown in all panels of Fig. 5.

**2.2. Calculation for  $^{242}\text{Pu}$ .** The next, lighter nucleus is  $^{242}\text{Pu}$ . As can be seen from Fig. 3 and Table 3, starting from spin  $I = 26^+$  an almost vertical line is realized for the moment of inertia as a function of the square of the rotational frequency. Obviously, this behavior is associated with band crossing. Neither the IBM phenomenology nor the VMI can reproduce this situation and the energies starting from the state with spin  $26^+$ . The calculation based on taking into account high-spin modes reproduces the state energies quite satisfactorily. The final band crossing occurs at spins  $28^+$ ,  $30^+$ . The calculated  $B(E2)$  values are shown in Fig. 5, where, as can be seen, no sharp decrease occurs, similarly to  $^{244}\text{Pu}$ . The smooth decrease in  $B(E2)$  is associated with the cutoff factor in the  $T(E2)$  transition operator.

Table 3. Comparison of experimental [15] and theoretical (Harris and IBM) excitation energies (in keV) for  $^{242}\text{Pu}$ . The IBM calculation uses  $\Omega = 24$

$I^\pi$	Exp.	$E_{\text{cal}}$	$E_{\text{cal}} - E_{\text{exp}}$	$E_{\text{IBM}}$	$E_{\text{IBM}} - E_{\text{exp}}$	$E_{\text{micr. IBM}}$	$E_{\text{micr. IBM}} - E_{\text{exp}}$
2 <sup>+</sup>	44.545(9)	44.655	0.11	44.523	-0.022	43.90	-0.64
4 <sup>+</sup>	147.4(1)	147.56	0.16	147.42	0.02	147.67	0.27
6 <sup>+</sup>	306.4(2)	306.19	-0.21	306.44	0.04	307.40	1.0
8 <sup>+</sup>	518.1(5)	517.38	-0.72	518.41	0.31	520.89	2.79
10 <sup>+</sup>	778.6(8)	777.70	-0.90	779.55	0.95	783.12	4.52
12 <sup>+</sup>	1084.0(4)	1083.66	-0.34	1085.8	1.8	1090.38	6.38
14 <sup>+</sup>	1431.7(16)	1431.60	-0.10	1433.2	1.5	1437.63	5.93
16 <sup>+</sup>	1817.4(4)	1817.70	0.30	1817.9	0.5	1825.31	7.91
18 <sup>+</sup>	2237.5(4)	2238.02	0.52	2236.5	-2	2242.08	4.58
20 <sup>+</sup>	2688.6(5)	2688.74	0.14	2686.4	-2.2	2690.98	2.38
22 <sup>+</sup>	3167.2(5)	3166.31	-0.89	3166.5	-0.7	3164.15	-3.05
24 <sup>+</sup>	3667.7(5)	3667.55	-0.15	3672.9	5.2	3660.16	-7.54
26 <sup>+</sup>	4180.2(6)	4189.73	9.5	4209.0	28.2	4168.47	-11.73
28 <sup>+</sup>	4691.2(8)	4730.54	39.3	4775.8	87.6	4681.14	-10.06
30 <sup>+</sup>	5201.2(11)	5288.03	86.8	5377.1	175.2	5194.36	-6.84
32 <sup>+</sup>	5723.9(11)	5860.55	137.5	6018.9	295	5721.56	-2.34

**2.3. Calculation for  $^{240}\text{Pu}$ .** For  $^{240}\text{Pu}$ , the IBM phenomenology gives a very successful description of states up to spin  $I = 30^+$ . For the state  $I = 32^+$ , the last one in the observed band, the difference between the calculated (IBM) and experimental energies is 10.4 keV (Table 4). In terms of the moment of inertia as a function of the square of the rotational frequency, this appears as upbending.

This situation is described by taking into account the interaction of collective states with high-spin modes, but it is necessary to implement a

Table 4. Comparison of experimental [15] and theoretical (Harris and IBM) excitation energies (in keV) for  $^{240}\text{Pu}$ . The IBM calculation uses  $\Omega = 25$

$I^\pi$	Exp.	$E_{\text{cal}}$	$E_{\text{cal}} - E_{\text{exp}}$	$E_{\text{IBM}}$	$E_{\text{IBM}} - E_{\text{exp}}$	$E_{\text{micr. IBM}}$	$E_{\text{micr. IBM}} - E_{\text{exp}}$
2 <sup>+</sup>	42.824(8)	42.852	0.028	42.835	0.011	42.32	-0.51
4 <sup>+</sup>	141.690(15)	141.712	0.022	141.470	-0.22	141.65	-0.04
6 <sup>+</sup>	294.319(24)	294.24	-0.078	294.22	-0.1	294.61	0.29
8 <sup>+</sup>	497.37(20)	497.28	-0.094	497.28	-0.09	498.75	1.38
10 <sup>+</sup>	747.4(3)	747.31	-0.093	747.39	0.0	750.23	2.83
12 <sup>+</sup>	1041.1(3)	1040.85	-0.25	1041.1	0.0	1045.20	4.10
14 <sup>+</sup>	1374.8(4)	1374.64	-0.16	1375.0	0.2	1380.93	6.13
16 <sup>+</sup>	1745.7(4)	1745.79	0.09	1746.2	0.5	1752.12	6.42
18 <sup>+</sup>	2151.6(5)	2151.77	0.17	2152.2	0.6	2158.41	6.81
20 <sup>+</sup>	2590.2(5)	2590.41	0.21	2590.7	0.5	2597.29	7.09
22 <sup>+</sup>	3059.8(6)	3059.9	0.1	3059.9	0.1	3066.66	6.86
24 <sup>+</sup>	3559.0(6)	3558.73	-0.27	3558.4	-0.6	3564.77	5.77
26 <sup>+</sup>	4086.3(6)	4085.66	-0.64	4085.2	-1.1	4093.38	7.08
28 <sup>+</sup>	4639.4(7)	4639.74	0.34	4639.6	-0.2	4641.94	2.54
30 <sup>+</sup>	5220.3(7)	5220.26	-0.04	5221.1	0.8	5221.96	1.66
32 <sup>+</sup>	5819.3(8)	5826.70	7.45	5829.7	10.4	5821.51	2.21

strong weakening of the corresponding interaction channels. The peculiarity of this nucleus is that, according to experimental data, the second derivative of the moment of inertia with respect to the square of the rotational frequency is negative, at least starting from spin  $22^+$  up to spin  $30^+$ , and then a sharp upbending occurs. At the same time, the collective component of the  $32^+$  state (Fig. 4) remains more than 70% collective, and band crossing has not occurred yet. However, the fact that in the theoretical calculation these interaction channels have to be strongly weakened suggests the influence of a four-quasiparticle state ( $j_{15/2}^4$ ) $^{(24^+)}$ . In this case, the collective state will have spin  $8^+$ . If this is the case, then what sometimes manifests itself as a second backbending may here become the precursor of the first.

Within the employed calculation scheme, four-quasiparticle modes are not considered, and all states retain a predominantly collective character. This leads to the corresponding behavior of  $B(E2)$ , shown in Fig. 5. Namely, it is an increase in  $B(E2)$  up to spin  $14^+$ , followed by a decrease.

**2.4. Calculation for  $^{238}\text{Pu}$ .** In the  $^{238}\text{Pu}$  nucleus, the moment of inertia from experimental data exhibits a linear dependence on the argument up to spin  $I = 22^+$ , and starting from spin  $I = 24^+$  a kink occurs in the dependence of this quantity. In [1], it was suggested that this is due to the influence of high-spin excitation modes, but without leading to band crossing. In the present work, results of calculations within the IBM phenomenology are presented with  $\Omega = 27$  in contrast to [1], where the results were given with  $\Omega = 24$ . The kink is not reproduced in either case. The VMI handles this. The microscopic calculation reproduces the experimental data reasonably well overall (Fig. 3, Table 5). The structure of the wave functions, shown in Fig. 4, demonstrates a smooth decrease in the collective component, with the

Table 5. Comparison of experimental [15] and theoretical (Harris and IBM) excitation energies (in keV) for  $^{238}\text{Pu}$ . The IBM calculation uses  $\Omega = 27$ , when taking into account high-spin states in the IBM, we adopted  $\Omega = 28$

$I^\pi$	Exp.	$E_{\text{cal}}$	$E_{\text{cal}} - E_{\text{exp}}$	$E_{\text{IBM}}$	$E_{\text{IBM}} - E_{\text{exp}}$	$E_{\text{micr. IBM}}$	$E_{\text{micr. IBM}} - E_{\text{exp}}$
$2^+$	44.065(15)	44.087	0.022	43.837	-0.23	43.07	-1.0
$4^+$	145.936(21)	145.847	-0.089	145.36	-0.58	144.85	-1.1
$6^+$	303.36(6)	303.06	-0.3	302.81	-0.55	302.41	-0.95
$8^+$	512.55(15)	512.85	0.3	513.64	1.09	513.23	0.68
$10^+$	771.9(5)	772.08	0.18	774.71	2.81	775.59	3.7
$12^+$	1077.7(5)	1077.64	-0.06	1082.5	4.8	1083.60	5.9
$14^+$	1426.4(6)	1426.48	0.08	1433.5	7.1	1432.66	6.26
$16^+$	1815.5(5)	1815.6	0.1	1823.8	8.3	1822.75	7.25
$18^+$	2241.7(6)	2242.03	0.33	2250.2	8.5	2249.4	8.2
$20^+$	2702.3(8)	2702.82	0.52	2709.2	6.9	2710.62	8.3
$22^+$	3195.4(8)	3195.11	-0.29	3198.1	2.7	3201.00	5.6
$24^+$	3717.1(10)	3716.11	-0.99	3714.3	-2.8	3719.14	2
$26^+$	4263.7(11)	4263.24	-0.46	4256.1	-7.6	4265.24	1.5
$28^+$	4833.3(13)	4834.09	0.79	4822.0	-11.3	4834.46	1.2
$30^+$	5426.5(9)	5426.51	0.01	5411.6	-14.9	5425.34	-1.2

Table 6. Comparison of experimental [15] and theoretical (Harris and IBM) excitation energies (in keV) for  $^{236}\text{Pu}$ . The IBM calculation uses  $\Omega = 28$

$I^\pi$	Exp.	$E_{\text{cal}}$	$E_{\text{cal}} - E_{\text{exp}}$	$E_{\text{IBM}}$	$E_{\text{IBM}} - E_{\text{exp}}$
$2^+$	44.63(9)	44.71	0.08	44.544	-0.09
$4^+$	147.45(9)	147.529	0.079	147.34	-0.11
$6^+$	305.80(10)	305.6	-0.2	305.82	—
$8^+$	515.70(22)	515.36	-0.34	516.31	0.61
$10^+$	773.5(3)	772.9	-0.6	774.44	0.9
$12^+$	1074.3(4)	1073.85	-0.45	1075.5	1.2
$14^+$	1413.6(4)	1413.41	-0.19	1414.6	1.0
$16^+$	1786.0(5)	1786.59	0.59	1787.1	1.1
$18^+$	2188.0(7)	2188.62	0.62	2188.6	0.6
$20^+$	2615.7(9)	2615.33	-0.37	2614.9	-0.8
$22^+$	3063.7(10)	3063.24	-0.46	3062.4	-1.3
$24^+$	3529.6(11)	3529.52	-0.08	3528.1	-1.5

maximum contribution from quasiparticle modes being 15% in the state with spin  $30^+$ . This is sufficient to reproduce the kink in the moment of inertia. The  $B(E2)$  values are shown in Fig. 5.

**2.5. Calculation for  $^{236}\text{Pu}$ .** For the  $^{236}\text{Pu}$  nucleus, the experimentally observed states extend only up to spin  $I = 24^+$ . These are the spins where, in this region of nuclei, high-spin modes have not become significant yet. Therefore, calculations were performed only within the VMI and the IBM phenomenology with  $\Omega = 27$ . The moments of inertia are shown in Fig. 3, and the energies are given in Table 6. The presented data are in good agreement with each other.

## CONCLUSIONS

Within the boson representation, an interpretation of the wave functions of the yrast bands in even-even Pu isotopes is given. For  $^{242,244}\text{Pu}$ , a band crossing at spins around  $I \simeq 24^+ - 28^+$  is reproduced. This corresponds to the replacement of the collective band by a band built mainly on a high-spin mode or a boson with angular momentum  $J = 12^+$ . It is important to note that the band replacement occurs onto the state  $b_{12^+}^+ |\psi_c(I_c)\rangle$  with  $I_c \geq 12^+$ , rather than with  $I_c = 0^+$ , as is the case in medium-mass nuclei from Xe to Ce and Dy [16]. In  $^{238}\text{Pu}$ , at spins  $I \geq 22^+$ , the influence of high-spin modes is important and manifests itself, although band crossing never occurs. For  $^{240}\text{Pu}$ , the situation remains not fully explained. This is evident from the behavior of the moment of inertia as a function of rotational frequency. In  $^{236}\text{Pu}$ , the description of level energies within the phenomenologies used is good up to the highest observed state with spin  $24^+$ .

In the cited works concerning the features of energies and moments of inertia of high-spin states ( $I \geq 22^+$ ), in addition to the traditional notions of “backbending” and the later “upbending”, we also employ the term “downbending”, which was introduced recently elsewhere. As research in this

direction progresses, the meaning of these terms undergoes some changes. To a lesser extent, this concerns the phenomenon of backbending, where a situation arises with  $J_1(\omega_1) < J_2(\omega_2 < \omega_1)$ , which is always accompanied by a band crossing. However, a case may also occur (as for  $^{242}\text{Pu}$ ), where  $J_1(\omega_1) < J_2(\omega_2 \simeq \omega_1) < J_3(\omega_3 \simeq \omega_1)$ , which is also accompanied by a band crossing. This case should also be classified as backbending. It should be noted that a band crossing can also occur in the absence of backbending, as demonstrated in [11, 13] for the nucleus  $^{222}\text{Th}$ . This is because the replacement of a collective band by a band built on a high-spin excitation mode occurs very gradually, from one spin to the next.

Regarding upbending, a sharp increase in the moment of inertia with increasing rotational frequency occurs. Our current opinion is as follows: if this effect can be reproduced within purely collective dynamics (e.g., by increasing the number of bosons  $\Omega$ , as in  $^{236}\text{Pu}$ ), then this case should not be classified as upbending. Conversely, if the additional growth of the function  $J(\omega)$  occurs due to the increasing influence of high-spin excitation modes (as in our case for  $^{238}\text{Pu}$ , albeit not to a pronounced degree), then such a case should be classified as upbending.

Finally, the downbending effect is associated with an additional increase in the energy of high-spin states. This effect manifests itself as a slowdown in the growth of  $J(\omega)$ , starting from a certain spin. It is most pronounced for  $^{238}\text{U}$  [13] and less pronounced for  $^{242}\text{Cm}$  [1]. Within the IBM framework, the effect is described by reducing  $\Omega$  compared to the values where the effect is not observed. It is not clearly manifested in Pu isotopes.

## REFERENCES

1. *Efimov A. D., Koval I. V., Izosimov I. N.* // Nucl. Phys. A. 2026. V. 1070. P. 123370.
2. *Edigo J. L., Ring P.* // J. Phys. G. 1982. V. 8. P. L43.
3. *Zhao Yue et al.* // Chin. Phys. Lett. 2012. V. 29. 052101.
4. *Afanasjev A. V., Abdurazakov O.* // Phys. Rev. C. 2013. V. 88. 014320.
5. *Jolos R. V., Donau F., Janssen D.* // Theor. Math. Phys. 1974. V. 20. P. 704.
6. *Arima A., Iachello F.* // Phys. Rev. Lett. 1975. V. 35. P. 1069.
7. *Harris S. M.* // Phys. Rev. B. 1965. V. 138. P. 509.
8. *Isakov V. I. et al.* // Eur. Phys. J. A. 2002. V. 14. P. 29.
9. *Efimov A. D.* // Phys. At. Nucl. 2020. V. 83. P. 651.
10. *Efimov A. D., Izosimov I. N.* // Phys. At. Nucl. 2023. V. 86. P. 333.
11. *Efimov A. D., Izosimov I. N.* // Int. J. Mod. Phys. E. 2025. V. 34. P. 2541004.
12. *Efimov A. D., Mikhajlov V. M.* // Bull. Russ. Acad. Sci.: Phys. 2013. V. 77. P. 862.
13. *Efimov A. D., Koval I. V., Izosimov I. N.* // Chin. Phys. C. 2025. V. 49. 074108.
14. *Efimov A. D., Mikhajlov V. M.* // Bull. Russ. Acad. Sci.: Phys. 2019. V. 83. P. 1136.
15. National Nuclear Data Center, Brookhaven National Laboratory. URL: <http://www.nndc.bnl.gov>.
16. *Efimov A. D., Izosimov I. N.* // Phys. At. Nucl. 2021. V. 84. P. 408.

Received on May 18, 2026.

Редактор *Е. И. Крупко*

Подписано в печать 24.06.2026.

Формат 60 × 90/16. Бумага офсетная. Печать цифровая.

Усл. печ. л. 1,00. Уч.-изд. л. 1,02. Тираж 90 экз. Заказ № 61329.

Издательский отдел Объединенного института ядерных исследований  
141980, г. Дубна, Московская обл., ул. Жолио-Кюри, 6.

E-mail: [publish@jinr.ru](mailto:publish@jinr.ru)  
[publish.jinr.ru](http://publish.jinr.ru)